

Radiochromic Semiconductive MOF with High Sensitivity and Fast Photochromic Response for Dual-mode X-ray Direct Detection

Xu-Ying Yu,^{a,b} Jia-Rong Mi,^a Qiu-Pei Qin,^{a,c} Xin-Ping Fang,^{a,c} Yong-Fang Han,^d Li-Zhen Cai,^a

Ming-Sheng Wang^{*a} and Guo-Cong Guo^{*a}

^a State Key Laboratory of Structural Chemistry, Fujian Institute of Research on the Structure of Matter, Chinese Academy of Sciences, Fuzhou, Fujian 3500608, P. R. China.

^b University of Chinese Academy of Sciences, Beijing 100049, P. R. China.

^c College of Chemistry and Materials Science, Fujian Normal University, Fuzhou, Fujian 350007, P. R. China.

^d College of Chemistry and Chemical Engineering, Liaocheng University, Liaocheng, Shandong 252000, P. R. China.

*Corresponding authors. E-mail addresses: mswang@fjirsm.ac.cn (M.-S. Wang),
gcguo@fjirsm.ac.cn (G.-C. Guo)

Experimental section:**Table S1.** Crystal and structure refinement data for **RCS-2** (as-synthesized).

RCS-2	
Formula	C ₃₉ H ₂₁ Dy ₂ NNa ₂ O ₃₀ S ₄
M _r	1482.79
Crystal system	monoclinic
Space group	C2/c
a (Å)	22.2834(2)
b (Å)	30.0518(3)
c (Å)	22.9729(3)
α (deg)	90
β (deg)	93.3340(10)
γ (deg)	90
V (Å ³)	15357.9(2)
D _{calcd} (g/cm ³)	1.283
Z	8
F(000)	5760.0
Abs coeff	12.000
R _{int}	0.0345
R ₁ ^a	0.0696
ωR ₂ ^b	0.1918
GOF on F ²	1.058
Δρ _{max} and Δρ _{min} (e/Å ³)	1.695 and -2.030

^aR₁ = Σ||F_o| - |F_c|| / Σ|F_o|, ^bωR₂ = {Σω[(F_o)² - (F_c)²]² / Σω[(F_o)₂]²}^{1/2}

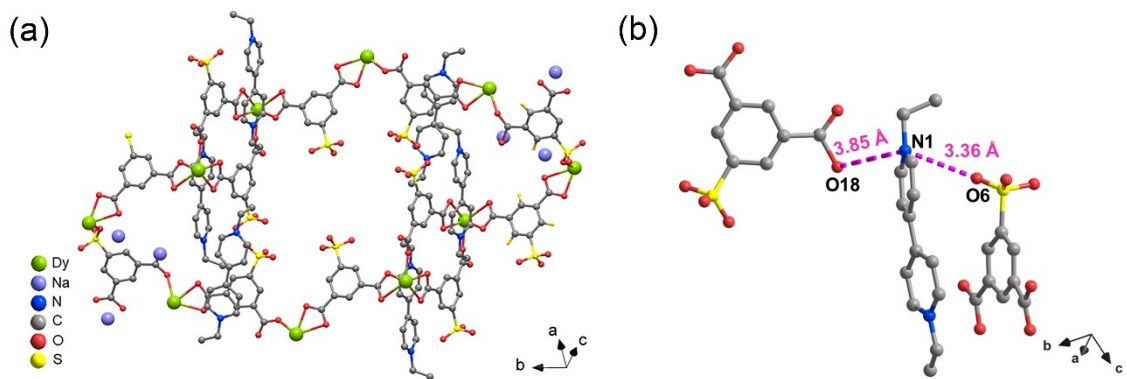


Fig. S1 Crystal structures for **RCS-2**: (a) One-dimensional pore structure formed by ligands and metals. (b) The distance of N and O atoms.

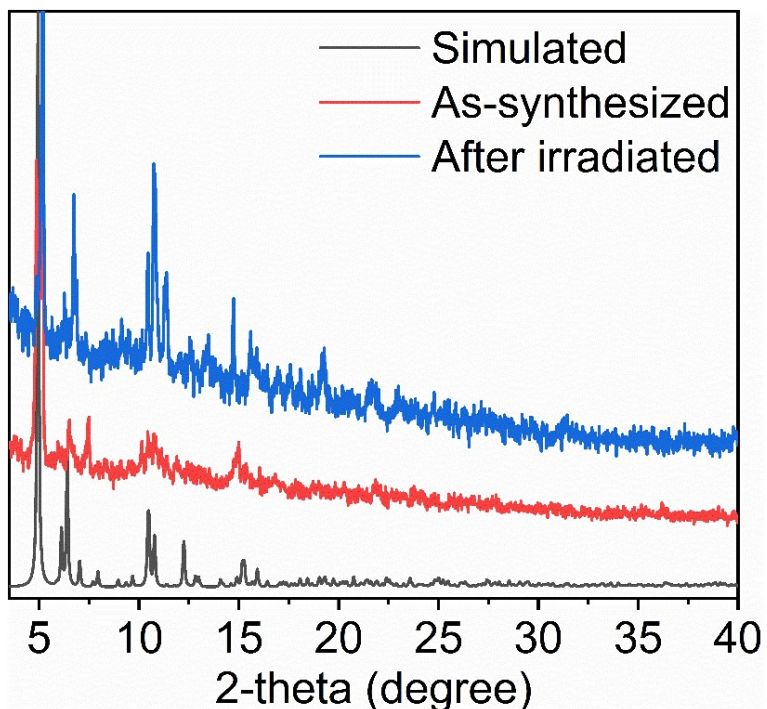


Fig. S2 PXRD for the as-synthesized sample and irradiated sample of **RCS-2**.

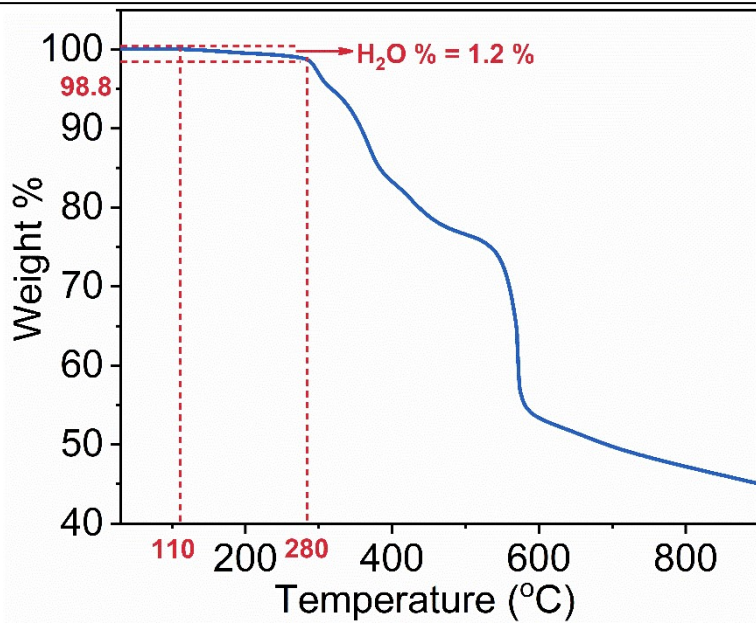


Fig. S3 TG curve for the as-synthesized sample of **RCS-2**.

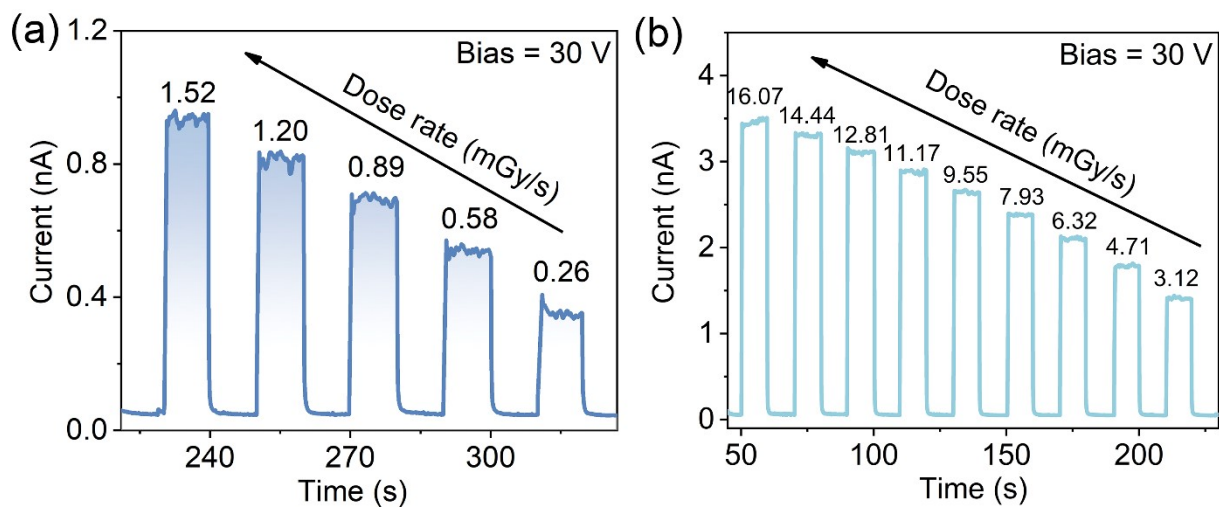


Fig. S4 The photocurrent of **RCS-2** versus time under different X-ray dose rates from 0.26 mGy/s to 1.52 mGy/s (a) and 3.12 mGy/s to 16.07 mGy/s (b).

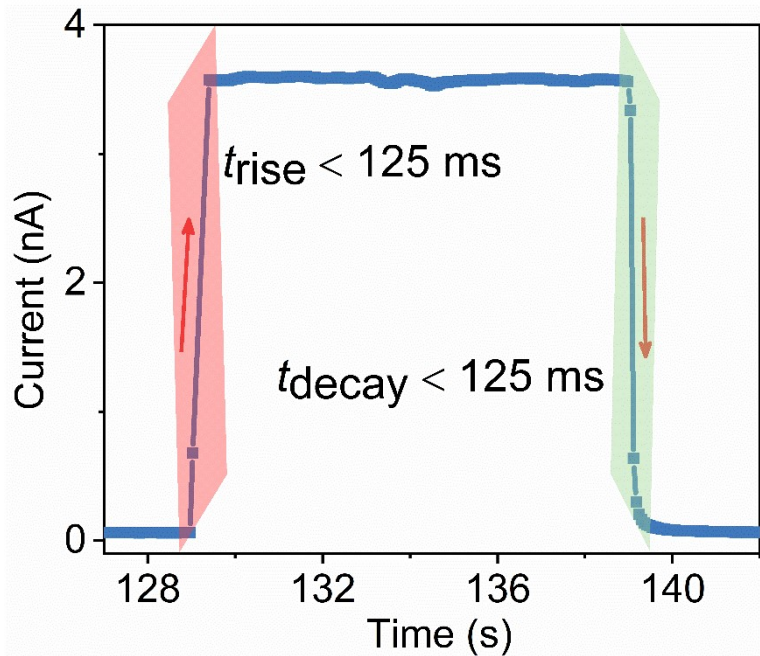


Fig. S5 Temporal response of RCS-2 with a bias voltage of 30 V.

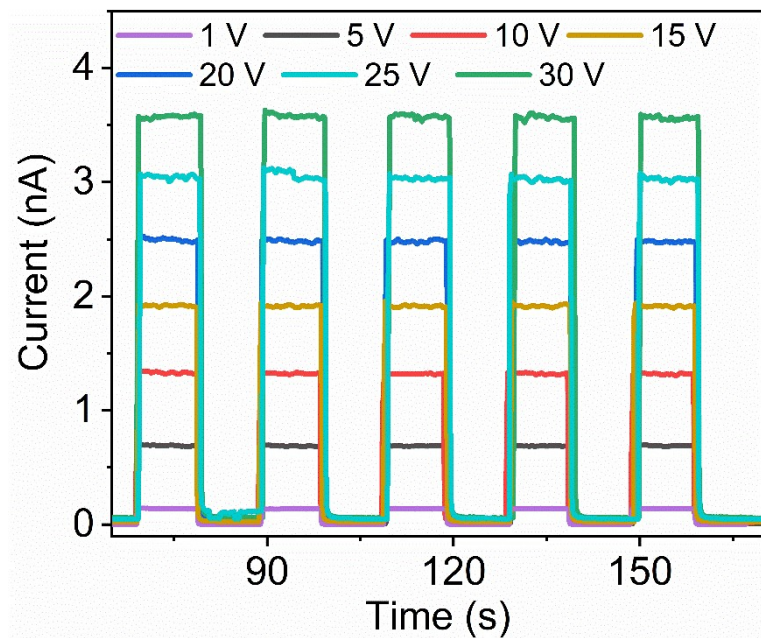


Fig. S6 X-ray induced photocurrent response of the RCS-2 detector under different bias voltage with the dose rate of $16.07 \text{ mGy}_{\text{air}} \text{ s}^{-1}$.



Fig. S7 Time-dependent color changes of crystalline samples upon irradiation of Al- K_{α} X-rays.

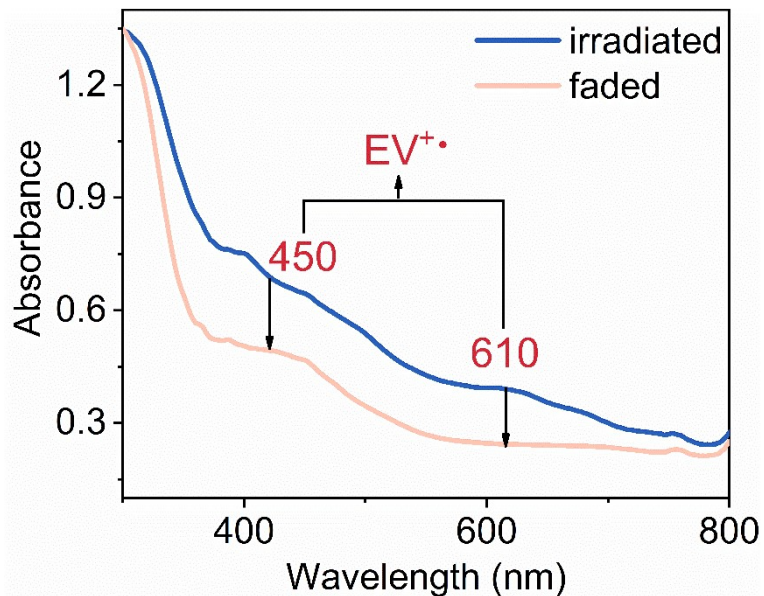


Fig. S8 Electronic absorption spectra of after irradiated and naturally faded sample for **RCS-2**.

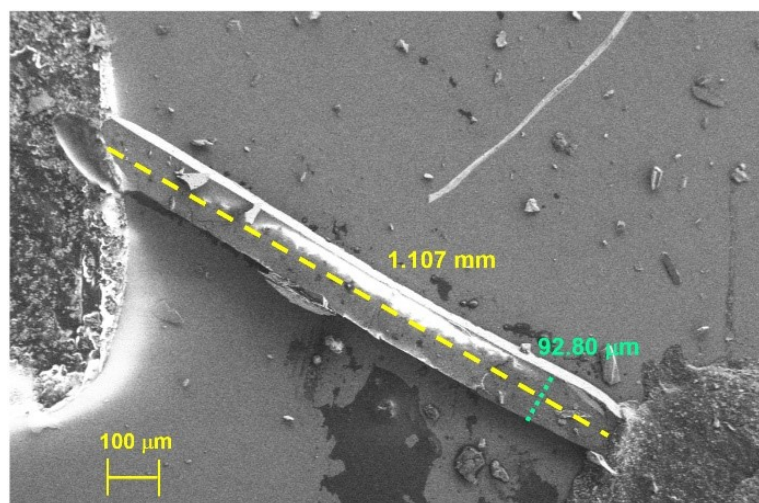


Fig. S9 SEM image of single-crystal detector for **RCS-2**.

supplementary information

Table S2. Summary and comparison of the direct X-ray detection performances for MOF and α -Se detectors.

Materials	Sensitivity (S , $\mu\text{CGy}^{-1}\text{cm}^{-2}$)	Bias voltage (V)	Mobility-lifetime product ($\mu\tau$, cm^2V^{-1})	Ref.
RCS-2 (SC.)	6385	30	1.61×10^{-4}	This work
RCS-1	98.58	30	5.32×10^{-4}	2
1-SC-a (SC.)	2697	30	3.44×10^{-4}	3
MOF-2-film	137.31	30	3.03×10^{-3}	4
Ni-MOF-film	98.6	10	3.26×10^{-4}	5
EV-MOF (SC.)	3216	30	8.27×10^{-6}	6
SCU-12	23.80	30	1.30×10^{-4}	7
SCU-13 (film)	65.86	100	4.31×10^{-4}	8
SCU-14	54.93	100	6.30×10^{-4}	9
RhB ⁺ @TbTATAB	51.90	100	1.12×10^{-3}	10
Cu-DABDT	78.70	1	6.49×10^{-4}	11
α -Se	20	5.50	10^{-7}	12

Single-crystal (SC.)

References:

1. G.M. Sheldrick, Crystal structure refinement with SHELXL, *Acta Cryst.* **2015**, C71, 3–8.
2. Yu, X.; Mi, J.; Han, Y.; Sun, C.; Wang, M.; Guo, G., A stable radiochromic semiconductive viologen-based metal–organic framework for dual-mode direct X-ray detection. *Chin. Chem. Lett.* **2023**, 109233.
3. Li, B.-Y.; Xie, M.-J.; Lu, J.; Wang, W.-F.; Li, R.; Mi, J.-R.; Wang, S.-H.; Zheng, F.-K.; Guo, G.-C., Highly Sensitive Direct X-Ray Detector Based on Copper(II) Coordination Polymer Single Crystal with Anisotropic Charge Transport. *Small* **2023**, 19 (42). DOI:10.1002/smll.202302492.
4. Xie, M.-J.; Lu, J.; Li, B.-Y.; Wang, W.-F.; Wang, S.-H.; Zheng, F.-K.; Guo, G.-C., Barium(II)-based semiconductive coordination polymers for high-performance direct X-ray detection and imaging: Reducing the exciton binding energy via enhancing π - π interactions. *Chem. Eng. J.* **2023**, 466, 143272.

supplementary information

5. Li, Z.; Chang, S.; Zhang, H.; Hu, Y.; Huang, Y.; Au, L.; Ren, S., Flexible Lead-Free X-ray Detector from Metal–Organic Frameworks. *Nano Lett.* **2021**, 21 (16), 6983-6989.
6. Han, Y.-F.; Xu, X.-M.; Wang, S.-H.; Wang, W.-F.; Wang, M.-S.; Guo, G.-C., Reusable radiochromic semiconductive MOF for dual-mode X-ray detection using color change and electric signal. *Chem. Eng. J.* **2022**, 437, 135468.
7. Wang, Y.; Liu, X.; Li, X.; Zhai, F.; Yan, S.; Liu, N.; Chai, Z.; Xu, Y.; Ouyang, X.; Wang, S., Direct Radiation Detection by a Semiconductive Metal–Organic Framework. *J. Am. Chem. Soc.* **2019**, 141 (20), 8030-8034.
8. Liang, C.; Zhang, S.; Cheng, L.; Xie, J.; Zhai, F.; He, Y.; Wang, Y.; Chai, Z.; Wang, S., Thermoplastic Membranes Incorporating Semiconductive Metal-Organic Frameworks: An Advance on Flexible X-ray Detectors. *Angew. Chem. Int. Ed.* **2020**, 59 (29), 11856-11860.
9. Cheng, L.; Liang, C.; Liu, W.; Wang, Y.; Chen, B.; Zhang, H.; Wang, Y.; Chai, Z.; Wang, S., Three-Dimensional Polycatenation of a Uranium-Based Metal-Organic Cage: Structural Complexity and Radiation Detection. *J. Am. Chem. Soc.* **2020**, 142 (38), 16218-16222.
10. Liang, C.; Cheng, L.; Zhang, S.; Yang, S.; Liu, W.; Xie, J.; Li, M. D.; Chai, Z.; Wang, Y.; Wang, S., Boosting the Optoelectronic Performance by Regulating Exciton Behaviors in a Porous Semiconductive Metal-Organic Framework. *J. Am. Chem. Soc.* **2022**, 144 (5), 2189-2196.
11. Li, Z.; Chang, S.; Zhang, H.; Hu, Y.; Huang, Y.; An, L.; Ren, S., Cu-based metal–organic frameworks for highly sensitive X-ray detectors. *Chem. Commun.* **2021**, 57 (69), 8612-8615.
12. Huang, H.; Abbaszadeh, S., Recent Developments of Amorphous Selenium-Based X-Ray Detectors: A Review. *IEEE Sens. J.* **2020**, 20 (4), 1694-1704.